

RNA polymerase motor on DNA track: effects of interactions, external force and torque

Tripti Tripathi,¹ Prasanjit Prakash,¹ and Debashish Chowdhury*¹

¹*Physics Department, Indian Institute of Technology, Kanpur 208016, India*

(Dated: March 6, 2019)

RNA polymerase (RNAP) is like a mobile molecular workshop that polymerizes a RNA molecule by adding monomeric subunits one by one, while moving step by step on the DNA template itself. Here we develop a theoretical model by incorporating their steric interactions and mechanochemical cycles which explicitly captures the cyclical shape changes of each motor. Using this model, we explain not only the dependence of the average velocity of a RNAP on the externally applied load force, but also predict a *nonmonotonic* variation of the average velocity on external torque. We also show the effect of steric interactions of the motors on the total rate of RNA synthesis. In principle, our predictions can be tested by carrying out *in-vitro* experiments.

PACS numbers: 87.16.Ac 89.20.-a

I. INTRODUCTION

Molecular motors [1] in living cells are either proteins or macromolecular complexes made of proteins and ribonucleic acids (RNAs). Like their macroscopic counterparts, these motors perform mechanical work, while translocating on a filamentous track, by converting input energy which is often supplied as chemical energy [1, 2, 3]. In this paper we study a special class of motors, called RNA polymerase (RNAP) which play crucial roles in gene expression [4].

Transcription of a gene encoded in the sequence of nucleotides in a specific segment of a DNA is carried out by RNAP motors which treat the DNA as a template [5]. An RNAP is more like a mobile workshop that performs three functions simultaneously: (i) it decodes the genetic message encoded in the template DNA and selects the appropriate nucleotide, the monomeric subunit of RNA, as dictated by the template, (ii) it catalyzes the addition of the monomeric subunit thus selected to the growing RNA molecule, (iii) it steps forward by one nucleotide on its template without completely destabilizing the ternary complex consisting of the polymerase, the template DNA and the product RNA. The free energy released by the polymerization of the RNA molecule serves as the input energy for the driving the mechanical movements of the RNAP. Therefore, these enzymes are also regarded as molecular motors [6].

During the transcription of a gene, the collective movement of the RNAPs on the same DNA track is often referred to as RNAP traffic because of its superficial similarity with vehicular traffic [7, 8]. The beginning and the end of the specific sequence corresponding to a gene are the analogs of the on-ramp and off-ramp of vehicular traffic on highways. The average number of RNAPs, which complete the synthesis of a RNA molecule per unit

time interval can be identified as the *flux* in RNAP traffic. Note that flux is the product of the number density and average velocity of the motors. Thus, flux in RNAP traffic is identical to the average rate of synthesis of the corresponding RNA. Using the terminology of traffic science [8], we'll call the relation between the flux and the number density of the motors as the *fundamental diagram*. The fundamental diagram is an important quantitative characteristic of traffic flow.

The dependence of the velocity of the motor on an externally imposed load (opposing) force is called the force-velocity relation which is one of the most important characteristics of a molecular motor. The force-velocity relation for RNAP motors have been measured by carrying out single molecule experiments [9, 10]. However, to our knowledge, the response of an RNAP motor to an externally applied torque has not been investigated so far. The effects of steric interactions of the RNAP motors on their dynamics has been studied only in a few experiments [11, 12, 13, 14, 15]; but, none of these addressed the question of the nature of the overall spatio-temporal organization of the RNAP motors in RNAP traffic.

The traffic-like collective dynamics of cytoskeletal molecular motors [16, 17, 18, 19, 20, 21] and that of ribosomes on mRNA tracks [22, 23, 24, 25, 26, 27, 28, 29, 30, 31, 32, 33] have been investigated theoretically in the physics literature. However, so far, RNAP traffic has received far less attention [39, 40, 41] In this paper we develop a model that captures not only the steric interactions between the RNAPs, but also separately the *biochemical reactions* catalyzed by an RNAP and the *cyclic shape changes* it undergoes during each mechano-chemical cycle. This model may be regarded as a “unified” description in the sense that the same model describes the single RNAP properties (e.g., the force-velocity and torque-velocity relations) as well as the collective spatio-temporal organization (and rate of RNA synthesis).

*Coresponding author; E-mail: debch@iitk.ac.in

II. BASIC MECHANO-CHEMISTRY AND THE MODEL

The main stages in the polymerization of polynucleotides by the polymerase machines are common:

(a) *initiation*: Once the polymerase encounters a specific sequence on the template that acts as a chemically coded start signal, it initiates the synthesis of the product. The RNAP, together with the DNA bubble and the growing RNA transcript, forms a “transcription elongation complex” (TEC). This stage is completed when the nascent product RNA becomes long enough to stabilize the TEC against dissociation from the template.

(b) *elongation*: During this stage, the nascent product gets elongated by the addition of nucleotides; during elongation [34], each successful addition of a nucleotide to the elongating mRNA leads to a forward stepping of the RNAP.

(c) *termination*: Normally, the process of synthesis is terminated, and the newly polymerized full length product molecule is released, when the polymerase encounters the *terminator* (or, stop) sequence on the template.

In this paper we are interested mainly in the elongation of the mRNA transcripts.

One of the key experimental observations is that an RNAP cycles between a “closed” and an “open” shape during each mechano-chemical cycle (see fig.1a) [35, 36, 37, 38]. Recognition of the correct incoming nucleotide (dictated by the template) and its binding with the catalytic site on the RNAP leads to its closing. It remains closed as long as the hydrolysis of the NTP takes place. The nascent RNA is elongated by one monomer on completion of this reaction which also produces pyrophosphate. Then, the shape of the RNAP switches back to its open shape from the closed one thereby facilitating release of the pyrophosphate. In the open shape, the RNAP is weakly bound to its DNA track and, in principle, can execute Brownian motion.

To our knowledge, none of the models of RNAP traffic reported earlier, explicitly capture these cyclic change of shape of the polymerase motor. Liverpool et al.[39] as well as Klumpp and Hwa [41] treat each RNAP as a rigid rod and describe its translocation from one nucleotide to the next on its template in terms of a single parameter. Thus, both these models capture the effects of the mechano-chemistry of individual RNAPs by an effective “hopping” rate constant. In an attempt to capture the most essential aspects of the mechano-chemical cycle of individual RNAP motors, we have assigned two possible “internal” states to an RNAP at each spatial position on its track [40]. However, each of these two states is, in reality, not a single bio-chemical state; a sequence of bio-chemical states which interconvert sufficiently rapidly are collectively represented by one “internal” state whereas the transition from one internal state to the other is the slowest of all the transitions and, therefore, rate-limiting. This minimal model neither distinguishes between purely chemical transitions pure shape changes, nor does it as-

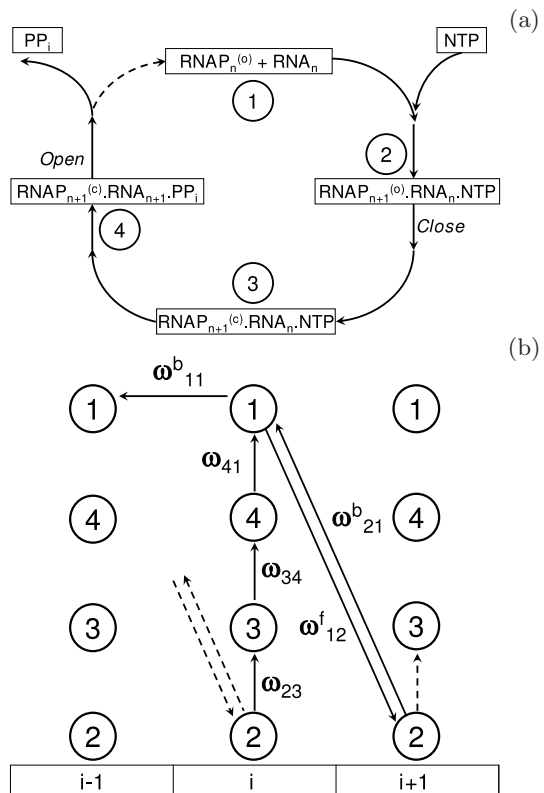


FIG. 1: A schematic representation of the mechano-chemical cycle of each RNAP in our model in the elongation stage is shown in (a). The labels $\dots, i-1, i, i+1, \dots$ in (b) denote the nucleotides on the DNA template. Thus, the horizontal direction in (b) denote positions of the RNAP while the vertical direction, at a given position, describe the corresponding “chemical” states.

sign distinct internal states to the “open” and “closed” shapes of the RNAP motor. Therefore, in this paper, we extend our earlier 2-state model to a 4-state model.

We shall use the terms RNAP and TEC interchangeably. We extend the 2-state model of ref.[40] by assigning four possible distinct “internal” state to the RNAP to capture its transitions between open and closed shapes. The composition of these four states and the spatial position of the RNAP as well as the transitions between these states are shown in fig.1.

III. RNAP TRAFFIC UNDER PERIODIC BOUNDARY CONDITION

In our model a one dimensional lattice of L sites represents the DNA template. Each site of these lattice corresponds to a single base pair. The total number of RNAP motors which move simultaneously on this template (and transcribe the same gene sequentially) is N ; the linear size of each RNAP is r in the units of base pairs. Therefore, the *number density* of the RNAP mo-

tors is $\rho = N/L$ whereas the corresponding *coverage density* is $\rho_{cov} = Nr/L$. The instantaneous spatial position of a RNAP is denoted by the leftmost site of the lattice it covers at that instant of time; however, it also “covers” all the adjacent $r - 1$ on the right side of the site which denotes its position. In order to capture the steric interaction (mutual exclusion) of the RNAPs, no site of the lattice is allowed to be covered simultaneously by more than one RNAP. Thus, this model of RNAP traffic may be regarded as a totally asymmetric simple exclusion process (TASEP) [42, 43] for hard rods each of which can exist in one of its four possible “intenal” states at any

arbitrary position on the lattice.

Let $P_\mu(i, t)$ denote the probability that there is a RNAP at the spatial position i and in the chemical state μ at time t . At any arbitrary site n and time t , these probabilities must satisfy the normalization condition

$$P(n, t) = \sum_{\mu=1}^4 P_\mu(n, t) = \frac{N}{L} = \rho \quad (1)$$

Under the mean-field approximation, the master equations for $P_\mu(i, t)$ are as follows:

$$\begin{aligned} \frac{dP_1(n, t)}{dt} = & P_1(n+1, t) \omega_{11}^b Q(n+1-r|\underline{n+1}) + P_2(n+1, t) \omega_{21}^b Q(n+1-r|\underline{n+1}) \\ & + P_4(n, t) \omega_{41} - P_1(n, t) \left[\omega_{11}^b Q(n-r|\underline{n}) + \omega_{12}^f Q(\underline{n}|n+r) \right] \end{aligned} \quad (2)$$

$$\frac{dP_2(n, t)}{dt} = P_1(n-1, t) \omega_{12}^f Q(\underline{n-1}|n-1+r) - P_2(n, t) \left[\omega_{21}^b Q(n-r|\underline{n}) + \omega_{23} \right] \quad (3)$$

$$\frac{dP_3(n, t)}{dt} = P_2(n, t) \omega_{23} - P_3(n, t) \omega_{34} \quad (4)$$

$$\frac{dP_4(n, t)}{dt} = P_3(n, t) \omega_{34} - P_4 \omega_{41} \quad (5)$$

where $Q(\underline{i}|j)$ is the conditional probability that, given an RNAP in site i , site j is empty. We calculate $Q(\underline{n}|n+r)$ following the same steps as we did in ref.[40], getting

$$Q(\underline{n}|n+r) = Q(n|\underline{n+r}) = \frac{1 - \rho r}{1 + \rho - \rho r} \quad (6)$$

The 4-state model reduces to our earlier 2-state model [40] in the limit $\omega_{23} \rightarrow \infty, \omega_{34} \rightarrow \infty$

In the steady state, all the $P_\mu(n, t)$'s become independent of time. Moreover, because of the periodic boundary conditions, all the sites are equivalent so that the steady-state probabilities $P_\mu(n)$'s are also independent of site index n . Solving Eqn.(2,3,4,5), together with normalization condition (1), in the steady state under periodic

boundary conditions, we get

$$P_1 = \rho \frac{\omega_{23} \omega_{34} \omega_{41} + \omega_{34} \omega_{41} \omega_{21}^b Q}{K} \quad (7)$$

$$P_2 = \rho \frac{\omega_{34} \omega_{41} \omega_{12}^f Q}{K} \quad (8)$$

$$P_3 = \rho \frac{\omega_{41} \omega_{12}^f \omega_{23} Q}{K} \quad (9)$$

$$P_4 = \rho \frac{\omega_{12}^f \omega_{23} \omega_{34} Q}{K} \quad (10)$$

Where;

$$\begin{aligned} K = & \omega_{23} \omega_{34} \omega_{41} + \omega_{34} \omega_{41} \omega_{21}^b Q + \omega_{34} \omega_{41} \omega_{12}^f Q \\ & + \omega_{41} \omega_{12}^f \omega_{23} Q + \omega_{12}^f \omega_{23} \omega_{34} Q \end{aligned} \quad (11)$$

The corresponding flux J is given by

$$\begin{aligned} J = & Q \left[\left(\omega_{12}^f - \omega_{11}^b \right) P_1 - \omega_{21}^b P_2 \right] \\ = & \frac{\rho Q}{K} \omega_{34} \omega_{41} \left[\omega_{12}^f \omega_{23} - \omega_{11}^b \omega_{23} - \omega_{11}^b \omega_{21}^b Q \right] \end{aligned} \quad (12)$$

Hence, the average velocity V of a single RNAP is given by

$$V = J/\rho = \frac{Q}{K} \omega_{34} \omega_{41} \left[\omega_{12}^f \omega_{23} - \omega_{11}^b \omega_{23} - \omega_{11}^b \omega_{21}^b Q \right] \quad (13)$$

The average velocity V depends on the number density ρ through the ρ -dependence of Q .

In the following subsections we'll use the formula (13) in the regime of sufficiently low coverage density ρ_{cov} to predict the dependence of V of single RNAP motors on external force and torque. Such dependences of V on external force and torque can be probed by carrying out single-molecule experiments *in-vitro*. In order to predict the total rate of RNA synthesis at coverage densities where steric interactions between the RNAPs is not negligibly small, we'll use the expression (12). Thus, our model may be regarded as a "unified" description of transcription in the sense that it can account for properties of single RNAP motors as well as their collective behaviour.

For numerical calculations, we use the rate constants extracted by Wang et al.[44] from the empirical data. In the absence of external force and torque, these rate constants are as follows:

$$\begin{aligned} \omega_{11}^b &= 9.4 \text{ s}^{-1} \\ \omega_{12}^f &= \omega_{12}^{f0} \cdot [NTP], \text{ with } \omega_{12}^{f0} = 10^6 \text{ M}^{-1} \cdot \text{s}^{-1} \\ \omega_{21}^b &= 0.21 \text{ s}^{-1} \\ \omega_{23} &= 100.0 \text{ s}^{-1} \\ \omega_{34} &= 1000.0 \text{ s}^{-1} \\ \omega_{41} &= 31.4 \text{ s}^{-1} \end{aligned} \quad (14)$$

A. Effects of externally applied force and torque

In this section we examine the effects of external force F and torque τ on the rate of RNA polymerization. From the force-velocity relation, we extract the stall force F_s , the load force which just stalls the a single RNAP motor. In order to extract these single RNAP properties from our model, we first use the formula (13) in the regime of extremely low coverage density of the RNAP motors.

1. Effects of external force

We assume that the load force F significantly affects only those steps of the mechano-chemical cycle of an RNAP which involve its mechanical movement, i.e., forward or backward movement in real space. Therefore, we assume that force-dependence of these rate constants are

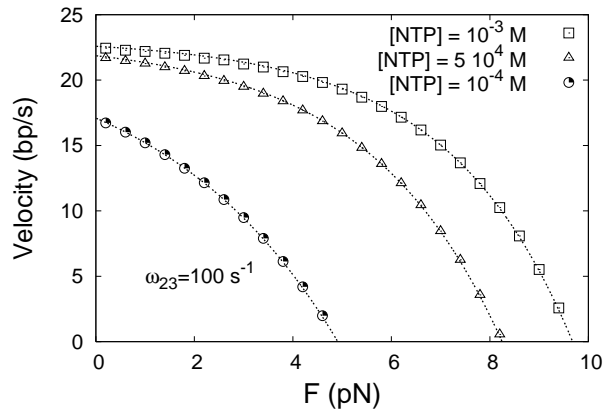


FIG. 2: The average speed of a single RNAP motor is plotted against the load force (a) for three different values of the NTP concentration. The lines have been obtained from the analytical expression (13) in extremely low number density of the RNAP motors. The discrete data points have been obtained by computer simulations of the model under identical conditions.

given by

$$\begin{aligned} \omega_{12}^f(F) &= \omega_{12}^f \exp(-F \delta/k_B T) \\ \omega_{21}^b(F) &= \omega_{21}^b \exp(F \delta/k_B T) \\ \omega_{11}^b(F) &= \omega_{11}^b \exp(F \delta/k_B T) \end{aligned} \quad (15)$$

where $\omega_{12}^f, \omega_{21}^b$ and ω_{11}^b are the corresponding values of the rate constants in the absence of the load force. In equation (15) the symbol $\delta = 0.34$ nm is the typical length of a single nucleotide. None of the rate constants other than the three listed in (15) are affected by the load force F .

The force-velocity relation of individual RNAP motors in our model is shown in fig.2 for three different concentrations of the NTPs. The average velocity decreases monotonically with increasing load force; the convex shape of the load-velocity curves are very similar to those reported by Wang et al. [44] in their single RNAP model. In this model, the higher is the NTP concentration the larger is the stall force F_s . Moreover, for a given load force $F < F_s$, the average velocity of the RNAP is larger at higher NTP concentration.

2. Effects of external torque

Now we consider the effects of an externally imposed torque which assists opening, but opposes closing of the *palm*-like shape of an isolated RNAP. These competing effects of the same torque on the two steps of each mechano-chemical cycle of individual RNAP motors has nontrivial effects on the rate of RNA synthesis. The above mentioned effects of the torque τ on opening and

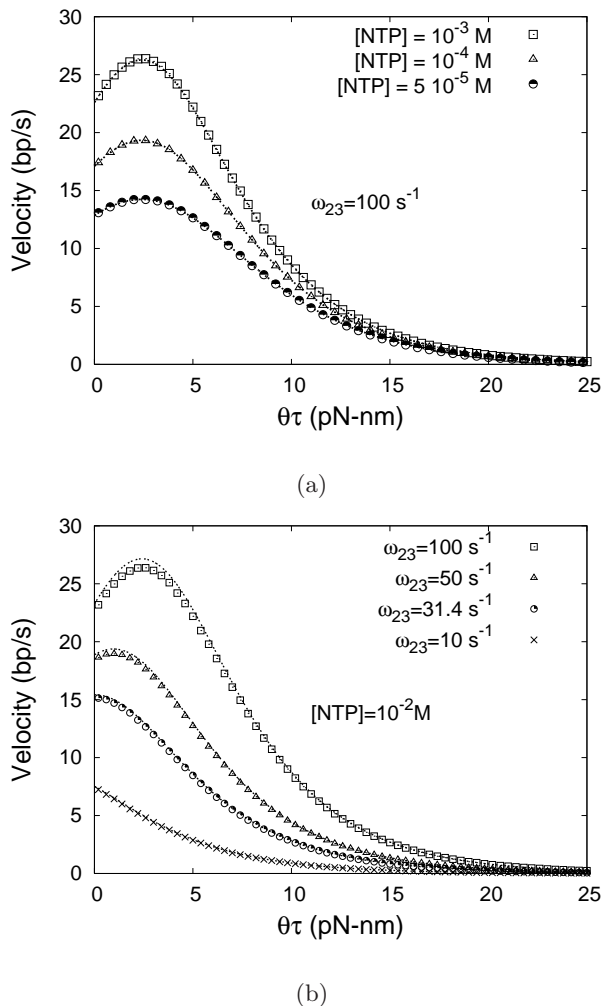


FIG. 3: The average speed of a single RNAP motor is plotted against the torque (a) for three different values of the NTP concentration for fixed $\omega_{23} = 100\text{s}^{-1}$, (b) for four different values of the rate constant ω_{23} , keeping NTP concentration fixed at $10^{-2}M$. The lines have been obtained from the analytical expression (13) at extremely low coverage density of the RNAP motors. The discrete data points have been obtained by computer simulations of the same model under identical conditions.

closing of RNAP are captured by the following choice of the correspondig rate constants

$$\begin{aligned}\omega_{23}(\tau) &= \omega_{23} \exp(-\tau \theta/k_B T) \\ \omega_{41}(\tau) &= \omega_{41} \exp(\tau \theta/k_B T)\end{aligned}\quad (16)$$

where ω_{23} and ω_{41} on the right hand sides of the equations are the rate constants in the absence of external torque.

The average velocity of the RNAP motors are plotted against the torque in fig.3 for different sets of values of the model parameters. The most dramatic effect of the torque is the *nonmonotonic* variation of V with τ in several experimentally accessible regimes of param-

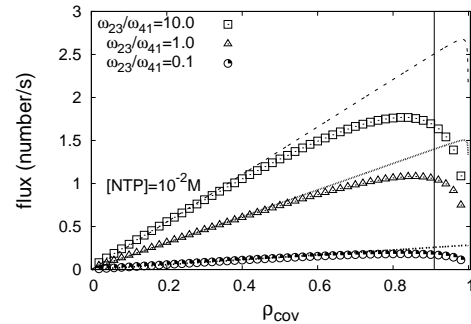


FIG. 4: The steady-state flux of the RNAPs, under periodic boundary conditions, plotted as a function of the coverage density ρ_{cov} for three different values of the ratio ω_{23}/ω_{41} . The vertical line represents the position of our theoretical estimate (17) of the maximum flux for fixed value of transition rates.

ter values. Increasing torque increases the opening rate and decreases the closing rate. As long as the opening rate is still lower (and, hence, rate limiting), the velocity increases with increasing torque. A peak appears where closing becomes the rate limiting step. In order to demonstrate the effect of this crossover from a regime dominated by opening to that dominated closing of RNAP, we have plotted one curve in fig.3(b) corresponding to $\omega_{23} = \omega_{41}$ for which the maximum occurs at $F = 0$.

B. Effects of steric interactions: flux-density relation

We have plotted mean-field estimate (12) of flux J against the coverage density ρ_{cov} in fig.4 for three different values of the ratio ω_{23}/ω_{41} at fixed NTP concentration of $10^{-2}M$. In the traffic science literature [8] such flux-density relations are usually referred to as the fundamental diagram. The qualitative features of the fundamental diagrams in fig.4 are similar to those observed earlier in the two state model of RNAP traffic [40]. The most notable feature of these fundamental diagrams is their *asymmetric shape*; this is in sharp contrast to the symmetry of fundamental diagram of a TASEP about $\rho = 1/2$. The physical reason for the asymmetric shape of the fundamental diagram in fig.4 is as follows: To get maximum current, system should have maximum number of particle-hole pairs. For $r = 1$, maximum number of particle hole pairs are when $1 - \rho = \rho$, $\rho = 0.5$. For $r \geq 2$, maximum number of particle-hole pairs can be found when $1 - \rho_m r = \rho_m$, i.e., $\rho_m = 1/(r + 1)$, which corresponds to

$$\rho_{cov}^m = r/(r + 1). \quad (17)$$

IV. RNAP TRAFFIC MODEL UNDER OPEN BOUNDARY CONDITION

For modeling transcription, the open boundary condition is more realistic than the periodic boundary conditions. Under this condition a RNAP can attach to start site (labeled as $n = 1$) with rate ω_α provided none of the

first r sites on the lattice is covered by any other RNAP. Similarly, after reaching the site $n = r$, an RNAP leaves the DNA track with rate ω_β . We calculate the conditional probability Q same way as we have done for the 2-state model of RNAP [40]. In this case, under mean-field approximation, the master equations for the probabilities $P_\mu(n, t)$ are given by

$$\begin{aligned} \frac{dP_1(n, t)}{dt} &= \omega_\alpha \left(1 - \sum_{s=1}^r P(s)\right) \delta(n-1) + \left[\omega_{11}^b P_1(n+1, t) + \omega_{21}^b P_2(n+1, t)\right] \left(1 - H(n-L)\right) Q^-(n+1) \\ &+ \omega_{41} P_4(n, t) - \omega_{11}^b P_1(n, t) H(n-2) Q^-(n) \\ &- \omega_{12}^f P_1(n, t) \left(1 - H(n-L)\right) Q^+(n) - \omega_\beta P_1(n, t) \delta(n-L) \end{aligned} \quad (18)$$

$$\begin{aligned} \frac{dP_2(n, t)}{dt} &= \omega_{12}^f P_1(n-1, t) H(n-2) Q^+(n-1) - \omega_{23} P_2(n, t) \\ &- \omega_{21}^b P_2(n, t) H(n-2) Q^-(n) \end{aligned} \quad (19)$$

$$\frac{dP_3(n, t)}{dt} = \omega_{23} P_2(n, t) - \omega_{34} P_3(n, t) \quad (20)$$

$$\frac{dP_4(n, t)}{dt} = \omega_{34} P_3(n, t) - \omega_{41} P_4(n, t) \quad (21)$$

Where $H(n)$ is the Heaviside step function defined by

$$H(n) = \begin{cases} 1 & \text{if } n \geq 0 \\ 0 & \text{if } n < 0. \end{cases} \quad (22)$$

and

$$Q^-(n) = \begin{cases} 1 & \text{if } n \leq r \\ \left(\frac{1 - \sum_{s=1}^r P(n-s)}{1 - \sum_{s=1}^r P(n-s) + P(n-r)}\right) & \text{if } n > r. \end{cases} \quad (23)$$

$$Q^+(n) = \begin{cases} 1 & \text{if } n > L - r \\ \left(\frac{1 - \sum_{s=1}^r P(n+s)}{1 - \sum_{s=1}^r P(n+s) + P(n+r)}\right) & \text{if } n \leq L - r. \end{cases}$$

We have numerically solved the mean-field equations (18)-(21) in the steady-state to compute the corresponding flux of the RNAP motors. These mean-field theoretic estimates of flux are compared with the corresponding data obtained from direct computer simulations of the model. These results are plotted as functions of the rate constants ω_α and ω_{12}^f , respectively, in figs.5 (a) and (b). The flux rises with increasing ω_{12}^f , but the rate of rise decreases with increasing ω_{12}^f . Eventually, the flux saturates because ω_{12}^f is no longer rate-limiting. This trend of variation of the total rate of RNA synthesis with the

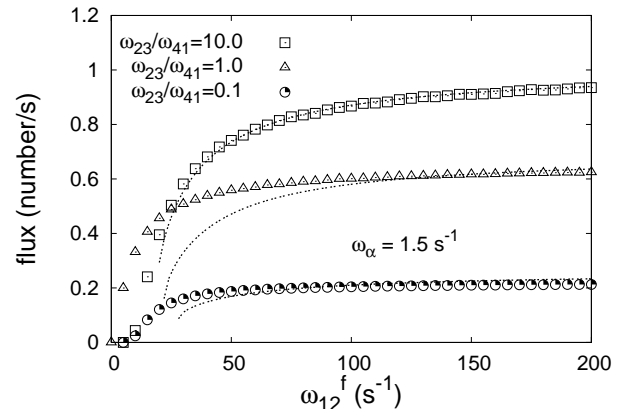


FIG. 5: The steady state current of RNAPs under open boundary condition for three different values of ratio ω_{23}/ω_{41}

concentration of NTP is similar to that observed earlier in our 2-state model of RNAP traffic [40]. Thus, a 2-state model of RNAP would be adequate to capture the dependence of the rate of RNA synthesis on the NTP concentration.

V. SUMMARY AND CONCLUSIONS

In this paper we have extended our earlier 2-state model of RNAP traffic to a 4-state model so as to capture some important cyclic shape changes in the mechanochemical cycle of each RNAP. The new model predicts the effects of these shape changes on the rate of RNA synthesis. Moreover, we have used the same model in the extremely low density limit to extract the force-velocity relation. Finally, we have demonstrated a novel non-monotonic variation of the average speed of the RNAP motors (and, hence, a nonmonotonic variation of the rate of synthesis of RNA) with the increase of an externally

imposed torque on the individual motors. In principle, it should be possible to test the new predictions of our model by carrying out laboratory experiments *in-vitro*.

In spite of some crucial differences, most of the polynucleotide polymerases seem to share a common “cupped right hand” architecture [45]. Therefore, it should be possible to make minor modifications in our 4-state model of RNAP so as to develop similar models of other polynucleotide polymerases.

Acknowledgements: This work is supported by a research grant from CSIR (India).

-
- [1] M. Schliwa, (ed.) *Molecular Motors*, (Wiley-VCH, 2003).
- [2] J. Howard, *Mechanics of motor proteins and the cytoskeleton*, (Sinauer Associates, 2001).
- [3] A.B. Kolomeisky and M.E. Fisher, in: *Annual Review of Physical Chemistry*, **58**, 675 (2007).
- [4] B. Alberts, D. Bray, K. Hopkin, A. Johnson, J. Lewis, M. Raff, K. Roberts and P.Walter, *Essential Cell Biology*, 2nd ed. (Garland Science, Taylor and Francis, 2004).
- [5] S. Borukhov and E. Nudler, *Trends Microbiol.* **16**, 126 (2008).
- [6] J. Gelles and R. Landick, *Cell*, **93**, 13 (1998).
- [7] D. Chowdhury, A. Schadschneider and K. Nishinari, *Phys. of Life Rev.* **2**, 318 (2005).
- [8] D. Chowdhury, L. Santen and A. Schadschneider, *Phys. Rep.* **329**, 199 (2000).
- [9] L. Bai, T.J. Santangelo and M.D. Wang, *Annu. Rev. Biophys. Biomol. Struct.* **35**, 343-360 (2006).
- [10] K.M. Herbert, W.J. Greenleaf and S.M. Block, *Annu. Rev. Biochem.* **77**, 149-176 (2008).
- [11] H. Bremer and M. Ehrenberg, *Biochim. Biophys. Acta* **1262**, 15 (1995).
- [12] V. Epshtein and E. Nudler, *Science* **300**, 801 (2003).
- [13] V. Epshtein, F. Toulme, A. Rachid Rahmouni, S. Borukhov and E. Nudler, *EMBO J.* **22**, 4719 (2003).
- [14] N. Crampton, W.A. Bonass, J. Kirkham, C. Rivetti and N.H. Thomson, *Nucleic Acids Research*, **34**, 5416 (2006).
- [15] K. Sneppen, I.B. Dodd, K.E. Shearwin, A.C. Palmer, R.A. Schubert, B.P. Callen and J.B. Egan, *J. Mol. Biol.* **346**, 399 (2005).
- [16] R. Lipowsky, Y. Chai, S. Klumpp, S. Liepelt and M. J.I. Miller, *Physica A* **372**, 34 (2006) and references therein.
- [17] E. Frey, A. Parmeggiani and T. Franosch, *Genome Inf.* **15**, 46 (2004) and references therein.
- [18] M.R. Evans, R. Juhasz and L. Santen, *Phys. Rev. E* **68**, 026117 (2003).
- [19] V. Popkov, A. Rakos, R.D. Williams, A.B. Kolomeisky and G.M. Schütz, *Phys. Rev. E* **67**, 066117 (2003).
- [20] K. Nishinari, Y. Okada, A. Schadschneider and D. Chowdhury, *Phys. Rev. Lett.* **95**, 118101 (2005).
- [21] P. Greulich, A. Garai, K. Nishinari, A. Schadschneider and D. Chowdhury, *Phys. Rev. E* **75**, 041905 (2007).
- [22] C. MacDonald, J. Gibbs and A. Pipkin, *Biopolymers* **6**, 1 (1968).
- [23] C. MacDonald and J. Gibbs, *Biopolymers*, **7**, 707 (1969).
- [24] G. Lakatos and T. Chou, *J. Phys. A* **36**, 2027 (2003).
- [25] L.B. Shaw, R.K.P. Zia and K.H. Lee, *Phys. Rev. E* **68**, 021910 (2003).
- [26] L.B. Shaw, J.P. Sethna and K.H. Lee, *Phys. Rev. E* **70**, 021901 (2004).
- [27] L.B. Shaw, A.B. Kolomeisky and K.H. Lee, *J. Phys. A* **37**, 2105 (2004).
- [28] T. Chou, *Biophys. J.*, **85**, 755 (2003).
- [29] T. Chou and G. Lakatos, *Phys. Rev. Lett.* **93**, 198101 (2004).
- [30] G. Schönherr and G.M. Schütz, *J. Phys. A* **37**, 8215 (2004).
- [31] G. Schönherr, *Phys. Rev. E* **71**, 026122 (2005).
- [32] J.J. Dong, B. Schmittmann and R.K.P. Zia, *J. Stat. Phys.* **128**, 21 (2007).
- [33] A. Basu and D. Chowdhury, *Phys. Rev. E* **75**, 021902 (2007)
- [34] S.M. Uptain, C.M. Kane and M.J. Chamberlin, *Annu. Rev. Biochem.* **66**, 117 (1997).
- [35] D. Temiakov, V. Patlan, M. Anikin, W.T. McAlister, S. Yokoyama and D.G. Vassilyev, *Cell* **116**, 381 (2004).
- [36] Y.W. Yin and T.A. Steitz, *Cell* **116**, 393 (2004).
- [37] Q. Guo and R. Sousa, *J. Mol. Biol.* **358**, 241 (2006).
- [38] S. Borukhov and E. Nudler, *Trends in Microbiol.* **16**, 126 (2008).
- [39] M. Voliotis, N. Cohen, C. Molina-Paris and T.B. Liverpool, *Biophys. J.* **94**, 334 (2007).
- [40] T. Tripathi and D. Chowdhury, *Phys. Rev. E* **77**, 011921 (2008).
- [41] S. Klumpp and T. Hwa, *PNAS* **105**, 18159 (2008).
- [42] B. Schmittmann and R.K.P. Zia, in: *Phase Transition and Critical Phenomena*, Vol. 17, eds. C. Domb and J. L. Lebowitz (Academic Press, 1995).
- [43] G. M. Schütz, in: *Phase Transitions and Critical Phenomena*, vol. 19 (Acad. Press, 2001).
- [44] H.Y. Wang, T. Elston, A. Mogilner and G. Oster, *Biophys. J.* **74**, 1186 (1998).
- [45] P. Cramer, *Bioessays* **24**, 724-729 (2002).
- [46] N. Korzheva and A. Mustaev, in ref.[1].